ROYAL SOCIETY
OF CHEMISTRY

PAPER

Check for updates

Sustainable synthesis of 1,4-disubstituted and *N*-unsubstituted 1,2,3-triazoles using reusable ZnO-CTAB nanocrystals†

Priyanuj Krishnann Hazarika,‡[a] Priyanka Gogoi,‡[a] Samprity Sarmah,[a] Babulal Das,[b] Kalyanjyoti Deori 🄳 *[a] and Diganta Sarma 🄳 *[a]

In this study, a sustainable and eco-friendly copper-free protocol has been developed for the regioselective synthesis of 1,4-disubstituted 1,2,3-triazoles using a zinc-based heterogeneous catalyst. This water-driven procedure links 1,4-disubstituted 1,2,3-triazoles in an azide–alkyne reaction *via* a one-pot multicomponent pathway without any base or reducing agents and ligands. The sonochemically prepared CTAB-stabilized ZnO particles with a nanorod-like architecture were quite robust and economical as a catalyst and could generate several 1,4-isomeric triazoles by tolerating different substituted azides and alkynes. Moreover, this catalyst was also applied for constructing pharmaceutically active *N*-unsubstituted 1,2,3-triazoles and 1,4,5-trisubstituted 1,2,3-triazoles with excellent yields. The catalyst was recovered and reused four times to synthesize 1,4-disubstituted and *N*-unsubstituted 1,2,3-triazoles. In addition, the successful two-gram-scale syntheses also confirm the efficiency of the catalyst. The catalytic protocol was designed considering green chemistry principles, and the eco-friendliness of this methodology was verified by its high eco-score and low *E*-factor values. This is the first report on using ZnO nanoparticles as a catalyst for regioselective triazole synthesis, and they are far better in terms of catalytic efficiency than many reported zinc-based catalysts.

Sustainability spotlight

In the recent years, 1,2,3-triazole containing medicinal scaffolds have emerged as a remedy against various life threatening diseases such as cancers, STDs and tuberculosis. The synthesis of these moieties generally requires harsh solvents, reducing agents, ligands and, most importantly, copper based metal catalysts. This has been a concern among the chemists as copper being cytotoxic can induce oxidative degradation of proteins, which causes cellular death in humans (when applied *in vivo*). Hence, in order to mitigate the harmful effects caused by the use of this metal, we have developed a zinc-based copper-free nanomaterial, ZnO-CTAB, for generating the 1,2,3-triazole derivatives. The synthesized heterogeneous nanocatalyst is quite sturdy, less toxic and can be easily prepared *via* sonochemical method. Water is used as an alternative medium for constructing the regioselective 1,4-disubstituted 1,2,3-triazoles. This mild protocol can tolerate various azides and alkynes bearing different functional groups in its moiety. With this methodology, we were able to synthesize few triazole derivatives that were earlier known to act as anti-bacterial agents and as IDO1 (indoleamine 2,3-dioxygenase) inhibitor in cancer immunotherapy. Moreover, the reusability of this catalyst is an added advantage as this can minimize the chemical wastes that are generated by the disposal of other non-recoverable catalysts. Our work emphasizes on the importance of the UN sustainable development goals: chemicals and waste (SDG 12, Responsible consumption and production) and health and populations (SDG 3, Good health and well-being).

Introduction

Heterocycles containing nitrogen in their skeletal structure possess remarkable biomedical properties that can potentially eliminate deadly diseases threatening human existence.[1–3] Five-membered aromatic 1,2,3-triazoles illustrate such heterocyclic moieties, which have the ability to imitate peptide bonds and oligosaccharides, enabling them to behave as antidotes against cancers, tumors, STDs and tuberculosis.[4–10] For instance, triazole-bearing medicinal hybrids, such as cefatrizine and tazobactam, have been approved as beta-lactam antibiotics against bacterial infections caused by drug-resistant ESKAPE pathogens.[11] A 1,4-disubstituted triazole, namely 3-(4-(4-phe-noxyphenyl)-1*H*-1,2,3-triazol-1-yl)benzo[*d*]isoxazole (PTB), works as an antiproliferative agent by restricting tubulin acetylation and thereby ceasing the proliferation of cancer cells in acute myeloid leukemia.[12] In addition to these pharmacological properties, 1,2,3-triazoles also display dynamic adequacy in the

[a]*Department of Chemistry, Dibrugarh University, Dibrugarh, Assam, 786004, India. E-mail: kalchemdu@gmail.com; dsarma22@gmail.com; dsarma22@dibru.ac.in; kalchemdu@dibru.ac.in*

[b]*Central Instruments Facility, Indian Institute of Technology Guwahati, Guwahati, 781039 Assam, India*

‡ Authors P. K. H and P. G. contributed equally.

industrial world as agrochemicals, fluorescent brighteners and anti-corrosive agents.[13]

The fascinating characteristics of these medicinal scaffolds have motivated chemists to devise methodologies for the synthesis of 1,2,3-triazoles. Originally established by Huisgen, the azide–alkyne thermal cycloaddition reaction marks the beginning of triazole synthesis.[14] Nevertheless, this was soon replaced by a copper-catalyzed 1,3-dipolar cycloaddition reaction because the former suffered from low regioselectivity, producing both 1,4- and 1,5-disubstituted 1,2,3-triazoles.[15,16] Despite the high regioselectivity of the CuAAC reaction, the use of copper has now been circumscribed because copper is cytotoxic and causes oxidative degradation of proteins when applied *in vivo*, leading to cellular damage in humans.[17] As such, copper-free protocols that utilize benign metal catalysts, such as $Zn(OAc)_2$,[18] Ag-graphene,[19] Ag–Al_2O_3@Fe_2O_3,[20] Ni–rGO–zeolite,[21] Raney Ni,[22] and CeO_2–Ag nanocomposites,[23] have been formulated to efficiently accomplish the AAC reaction.[24–26] However, except for a few sustainable methodologies[27,28] that exist in the literature, the majority of protocols rely on volatile organic solvents, high temperatures, reducing agents or additives, and involve long reaction times and complicated catalyst preparation techniques, which reduce the applicability of these protocols in biochemical fields. These drawbacks have asserted the need for new protocols to obtain the desired compounds in a more sustainable way.

Zinc-based nanomaterials form the foundation of many organic syntheses as they can enhance the reactions and generate tremendous yields owing to their superior surface area, good selectivity and reusability.[29–34] Hence, we have focused on developing a sustainable, copper-free nanostructured material in this work. Zinc oxide is a preferred material for this purpose because it is an economical, biodegradable and highly stable heterogeneous catalyst.

Here, a simple sonochemical method was developed to synthesize a nanostructured ZnO catalyst stabilized with CTAB (cetyltrimethylammonium bromide) as the surfactant. This newly synthesized nanocatalyst was employed, for the first time, to synthesize 1,4-disubstituted 1,2,3-triazole; it produced a single isomer with an excellent yield. However, when non-supported ZnO NPs were used for the 1,3-dipolar cycloaddition reaction, an inadequate yield (60%) was obtained and both 1,4- and 1,5-isomers were generated in an 80:20 ratio. This implies that CTAB not only acts as a stabilizer here but also helps in influencing the yield and maintaining the selectivity of the AAC reaction. In addition to 1,4-disubstituted 1,2,3-triazoles, the ZnO-CTAB nanocatalyst also facilitated the synthesis of N-unsubstituted 1,2,3-triazoles with outstanding yields (65–96%) *via* a one-pot multicomponent reaction system.

Results and discussion

A single-step sonication procedure, in which ultrasonic irradiation controlled the rate of nucleation and formation of the ZnO nanocrystals, was developed. CTAB was used here to control crystal growth and prevent the coagulation of the nanoparticles, thereby stabilizing its interface (Scheme 1).

The crystal structure and the morphology of the newly designed nanocrystals were studied by powder X-ray diffraction (PXRD) and transmission electron microscope (TEM) analyses, respectively. The PXRD pattern of the as-synthesized ZnO-CTAB showed peaks at 2θ values 31.72, 34.34, 36.18, 47.54, 56.56, 62.88, 66.58, 67.90 and 68.86°, which are well in agreement with the standard pattern of bulk ZnO (JCPDS no. 5-0664; crystal structure – hexagonal, wurtzite). However, the intensity ratios of the peaks were not consistent with the XRD pattern of bulk ZnO, which suggests that crystal growth towards a specific direction may be controlled by the CTAB surfactant (Fig. 1).

As observed in the low-magnification TEM image (Fig. 2), a rod-like architecture of ZnO was visualized. The high-resolution transmission electron micrograph (HRTEM) of the rods revealed clear lattice fringes with an interplanar d-spacing of 0.258 nm, which corresponds with the (002) planes of ZnO. The corresponding selected area electron diffraction (SAED) pattern featured bright twinkling spots that depict the highly crystalline nature of the nanomaterial (Fig. 2). All the constituent elements were distributed evenly within the crystal, as visualized in the elemental mappings obtained using high-angle annular dark field-scanning transmission electron microscopy (HAADF-STEM) (Fig. 3).

X-ray photoelectron spectroscopy (XPS) was performed in order to evaluate the oxidation state of Zn present in the material. In Fig. 4, the Zn spectrum displays two doublets at binding energy values 1021.01 eV and 1044.11 eV, corresponding to the $Zn\ 2p_{3/2}$ and $Zn\ 2p_{1/2}$ states, respectively.
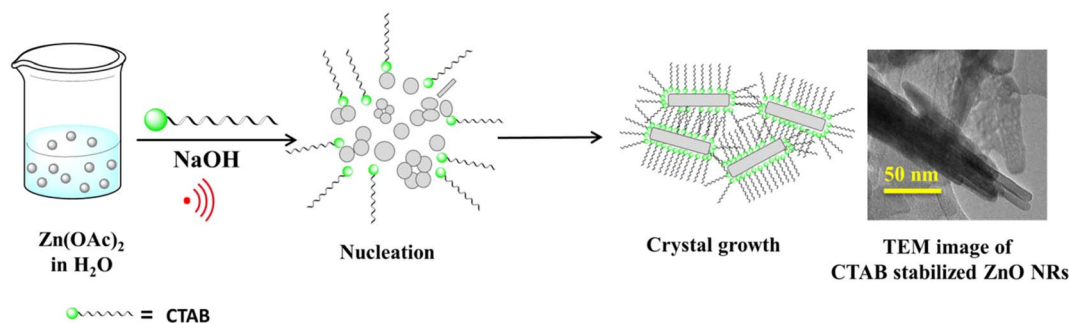
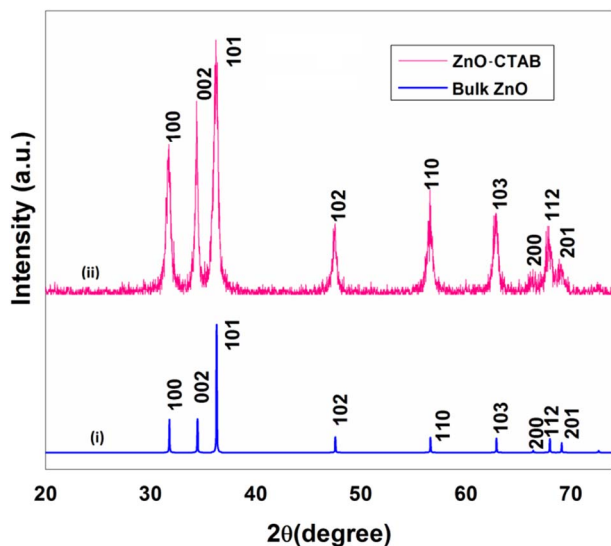**Scheme 1** Role of CTAB in the synthesis of the ZnO-CTAB nanocatalyst.

Fig. 1 PXRD patterns of (i) bulk ZnO and (ii) the as-synthesized ZnO-CTAB sample.

The energy spacing between the two peaks was found to be 23.10 eV, which signifies the presence of Zn in the +2 oxidation state. The oxygen 1 s spectrum showed a peak at 529.90 eV, matching the standard data. The low-resolution survey scan contained the 1s states of oxygen and carbon and the 2p states of Zn. Zinc loading in the catalyst was determined by inductively coupled plasma mass spectrometry (ICP-MS) and was found to be 16.83 wt%.

In this work, the catalytic performance of the newly synthesized ZnO-CTAB catalyst toward the synthesis of different types of 1,2,3-triazole derivatives was investigated. The results demonstrate that the procedure worked incredibly well for the synthesis of both 1,4-disubstituted and 1,4,5-tri substituted 1,2,3-triazoles from their respective alkynes in aqueous solvents. Moreover, the protocol was also applicable to the synthesis of N-unsubstituted triazoles.

For synthesizing 1,4-disubstituted 1,2,3-triazoles, benzyl azide and phenylacetylene were selected as the prime substrates and were reacted at 60 °C in water in the presence of 50 μL of ethylene glycol (EG). Initially, different zinc salts were examined for comparison with the as-synthesized catalyst; however, these salts, *viz.* $ZnSO_4$, $ZnCl_2$ and zinc acetate, failed to maintain regioselectivity and both the triazole isomers (1,4- and 1,5-isomers) were formed in an uncontrolled manner (Table 1, entries 2–4). Moreover, pure zinc metal (Zn dust) was employed, which produced only 40% of the desired product (Table 1, entry 8). The inclusion of 5 mg of the developed ZnO-CTAB catalyst to
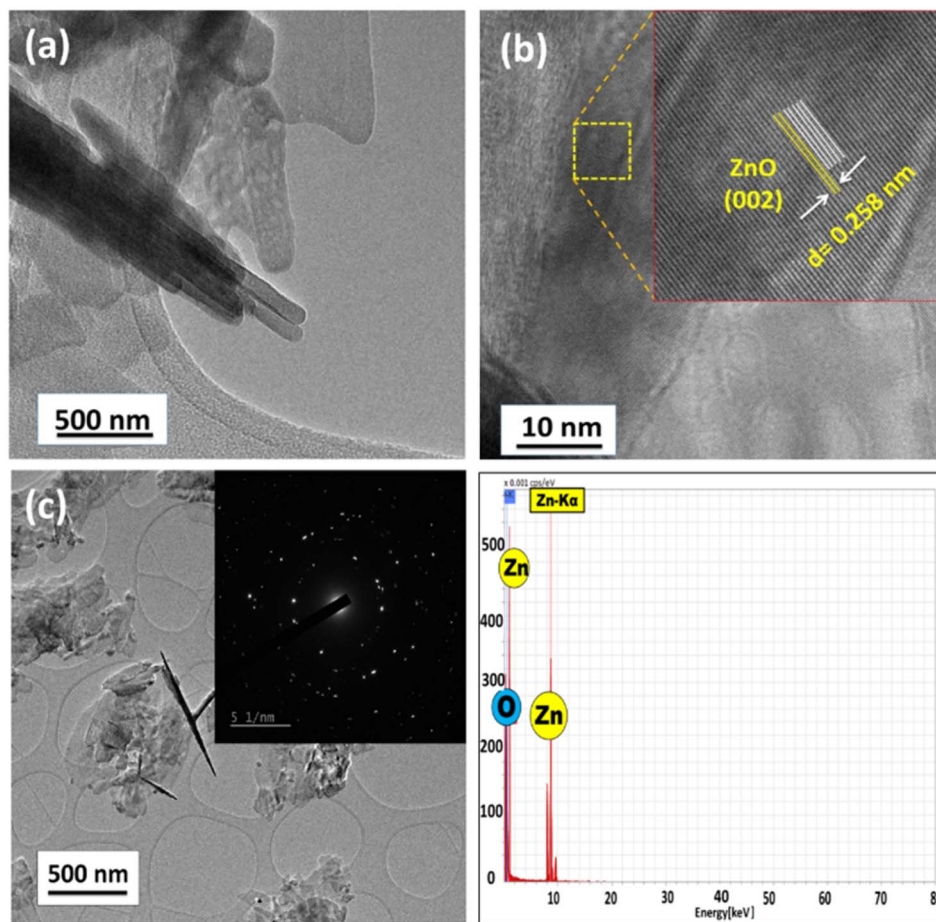

Fig. 2 (a) Low-resolution TEM micrograph, (b) phase contrast HR-TEM image, (c) TEM image with the SAED pattern as the inset and (d) TEM-EDS spectrum of the as-synthesized ZnO-CTAB nanocrystal.
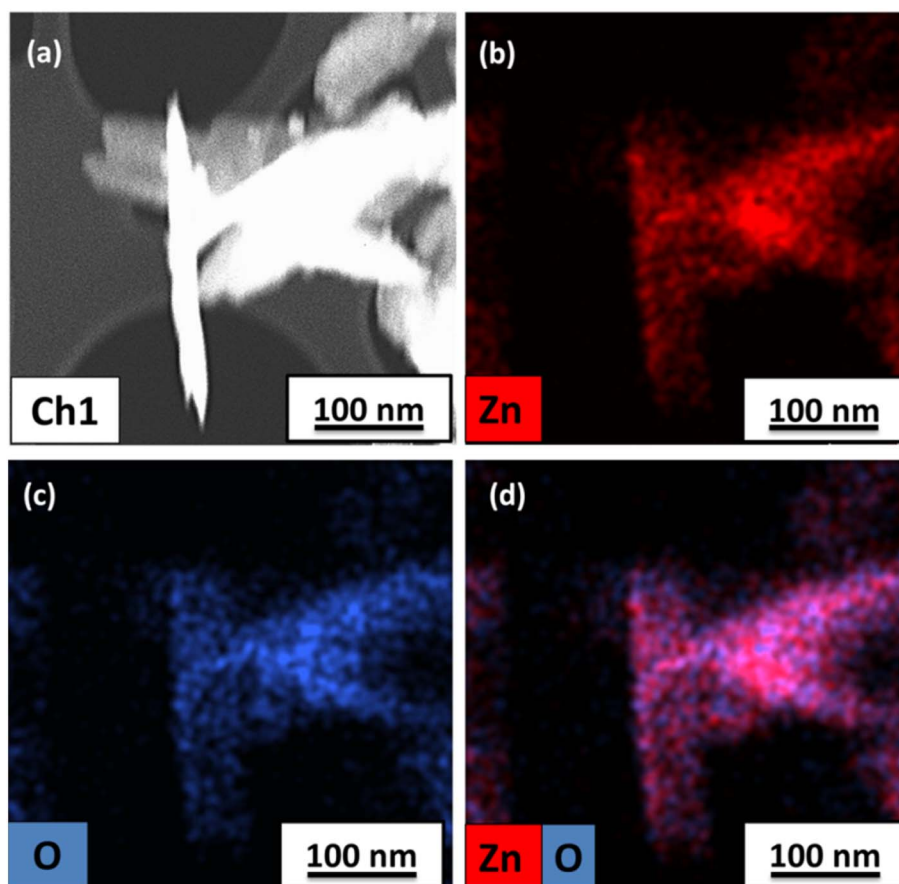
Fig. 3 (a) STEM image and elemental mappings of (b) Zn, (c) O and (d) both Zn and O in the as-synthesized ZnO-CTAB nanocrystals.

the reaction system generated the 1,4-isomer as a solitary product with outstanding yields (99%) (Table 1, entry 6). Simply heating the substrates in the absence of the catalyst produced both isomers in a 60 : 40 ratio with only 30% substrate conversion, ruling out the possible formation of a single isomer under thermal conditions without using the requisite catalyst (Table 1, entry 7). We carried out the azide–alkyne reaction using commercial zinc oxide, which afforded lower conversion with isomer formation in the ratio of 80 : 20 (Table 1, entry 1).

The effect of solvents was further demonstrated by screening a range of polar and non-polar solvents, and it was found that the water-ethylene glycol mixture was the best solvent for the complete conversion of the precursors (Table 2, entry 11). Other solvents, such as ethanol, methanol, toluene, DMF (dimethyl formamide) and DMSO (dimethyl sulfoxide), were not suitable for the catalytic system as they were unsuccessful in sustaining the yield percentage and regioselectivity of the products (Table 2). The addition of a small amount of ethylene glycol to water was necessary as it ensured complete dissolution and hence better interaction between the precursors.

After standardizing the ideal solvent, temperature variation was further employed in order to find the optimum temperature required for the reaction. Initially, 80 °C was selected for performing the reaction but it outweighed the regioselective nature of the catalyst and resulted in the generation of both isomers

(Table 2, entry 9). Reducing the temperature to 60 °C resulted in a single isomeric triazole in 3 h (Table 2, entry 11). At room temperature, a 30% product yield was obtained, which did not rise even after reacting for 24 h and increasing the catalyst amount (Table 2, entry 14).

Eventually, after optimizing the reaction conditions, we assessed the efficiency of the catalyst with different azides and alkynes. Benzyl azides containing chloro-, nitro-, bromo-, trifluoromethyl- and trifluoromethoxy-groups at the para position formed 1,4-isomer as the major product with 85–99% yields when reacted with phenylacetylene (Schemes 2 and **3a–f**). The reaction of 3,5-bis(3,5-dimethoxybenzyloxy)benzylazide with phenylacetylene required more time, which may be because of steric hindrance imposed by the bulky azide (Scheme 2 and **3g**). A single-crystal X-ray diffraction analysis was carried out for one of the triazole molecules (Scheme 2 and **3d**) in order to ensure the formation of only the 1,4-isomeric product (ESI, Fig. S2†).[42]

Next, aromatic alkynes containing different functional groups were explored, and it was observed that both the electron-donating and -withdrawing groups present in alkynes reacted efficiently with their corresponding azides (Scheme 3). Both functionalized and non-functionalized aliphatic alkynes, such as ethyl propiolate, propargyl alcohol and octyne, reacted smoothly under the optimized condition (Scheme 3, **6o, 6l** and **6n**). Moreover, the triazole derivative 4-((1-(4-chlorobenzyl)-1*H*-

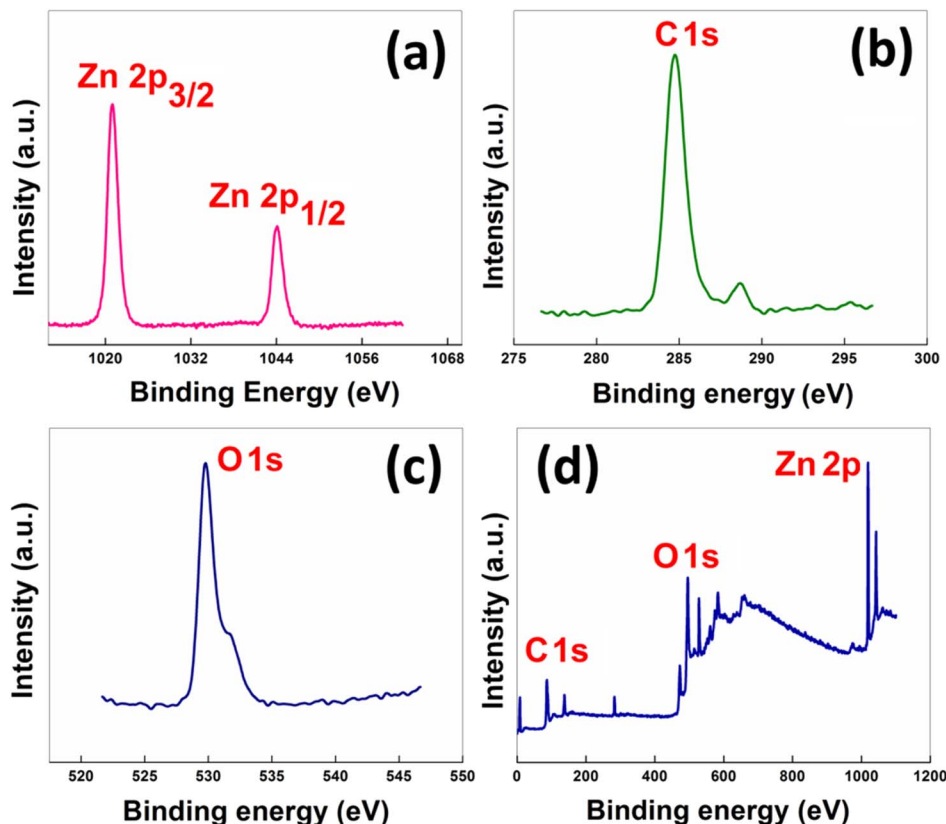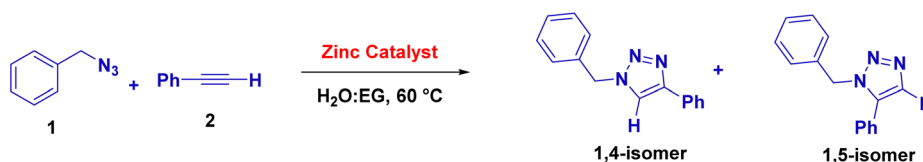**Fig. 4** High-resolution XPS spectra of the as-synthesized nanocatalyst: (a) Zn 2p, (b) C 1s (c) O 1s and (d) the wide survey scan.

Table 1 Optimization of the catalyst for the synthesis of 1,4 disubstituted 1,2,3-triazoles[a]

Entry	Catalyst	Amount (mg)	1,4-:1,5-isomer ratio	% yield[b]
1	ZnO commercial	15	80:20	60
2	$ZnSO_4$	15	50:50	60
3	$ZnCl_2$	15	60:40	70
4	Zinc acetate	15	60:40	70
5	ZnO-CTAB	3	100:0	90
6	ZnO-CTAB	5	100:0	99
7	Without catalyst	—	60:40	30
8	Zn metal (Zn dust)	5	60:40	30

[a] Reaction conditions: benzylazide (1 mmol), phenylacetylene (1.2 mmol), H_2O:EG (3 mL) with different zinc sources at 60 °C, 3 h. [b] Isolated yield.

1,2,3-triazole-4-yl)methoxy)-3-methoxybenzaldehyde, which is well-known as an anti-bacterial agent, could be successfully synthesized using our protocol (Scheme 3 and **6v**).[35]
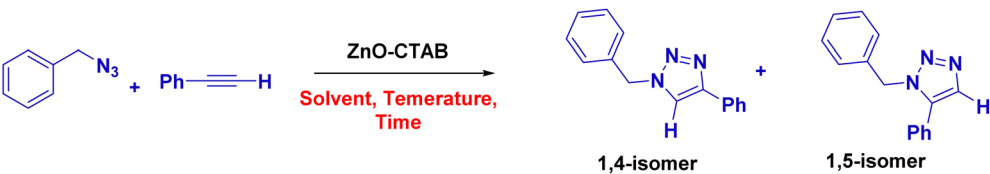
The catalyst was also capable of forming 1,4-regioselective triazoles *via* the one-pot three-component reaction of benzyl bromides, sodium azide and aromatic alkynes. The corresponding products were formed with 75–90% yields (Scheme 4 and **9a–h**).

In order to explore the potentiality of the as-synthesized catalyst in other reactions, it was further employed for the synthesis of *N*-unsubstituted triazoles (Scheme 5). The one-pot reaction was executed using aromatic aldehydes, sodium azide and nitromethane, which were heated at 80 °C in DMSO. This protocol

Paper

Table 2 Solvent and temperature optimization for the synthesis of 1,4 disubstituted 1,2,3-triazoles[a]


Entry	Solvent	Temperature [°C]	Time [h]	1,4- : 1,5- isomer ratio	% yield[b]
1	Ethanol	70	16	90 : 10	20
2	Methanol	70	16	90 : 10	10
3	DMSO	60	16	80 : 20	10
4	DMF	60	16	80 : 20	10
5	H_2O	60	16	50 : 50	50
6	H_2O/t-BuOH (1 : 1)	60	16	70 : 30	70
7	Ethylene glycol	60	16	80 : 20	70
8	PEG-400	80	16	60 : 40	40
9	H_2O-EG (6 : 1)	80	3	90 : 10	99
10	H_2O-EG (6 : 1)	60	6	100 : 0	99
11	H_2O-EG (6 : 1)	60	3	100 : 0	99
12	H_2O-EG (1 : 6)	60	16	100 : 0	50
13	H_2O-EG (4 : 2)	60	16	100 : 0	80
14	H_2O-EG (6 : 1)	25	24	100 : 0	30
15	Acetonitrile	60	16	60 : 40	25
16	DCM	60	6	60 : 40	20
17	Toluene	70	10	60 : 40	30
18	DCE	60	10	60 : 40	20
19	No solvent	60	24	60 : 40	30

[a] Reaction conditions: benzylazide (1 mmol), phenylacetylene (1.2 mmol), H_2O:EG (3 mL), and catalyst (5 mg). [b] Isolated yield.
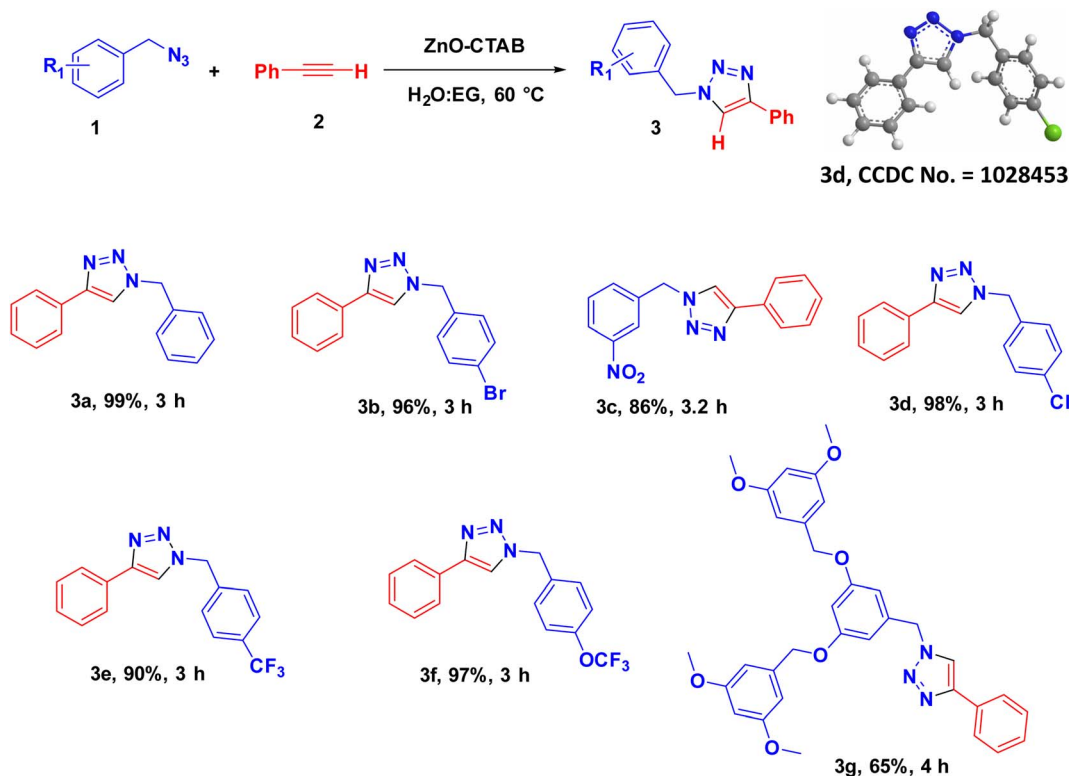
Scheme 2 Cycloaddition of aromatic azides and phenylacetylene catalyzed by ZnO-CTAB. [a]Reaction conditions: azide (1 mmol), phenyl-acetylene (1.2 mmol), H_2O:EG (3 mL), and catalyst (5 mg). All yields are reported as isolated yield.
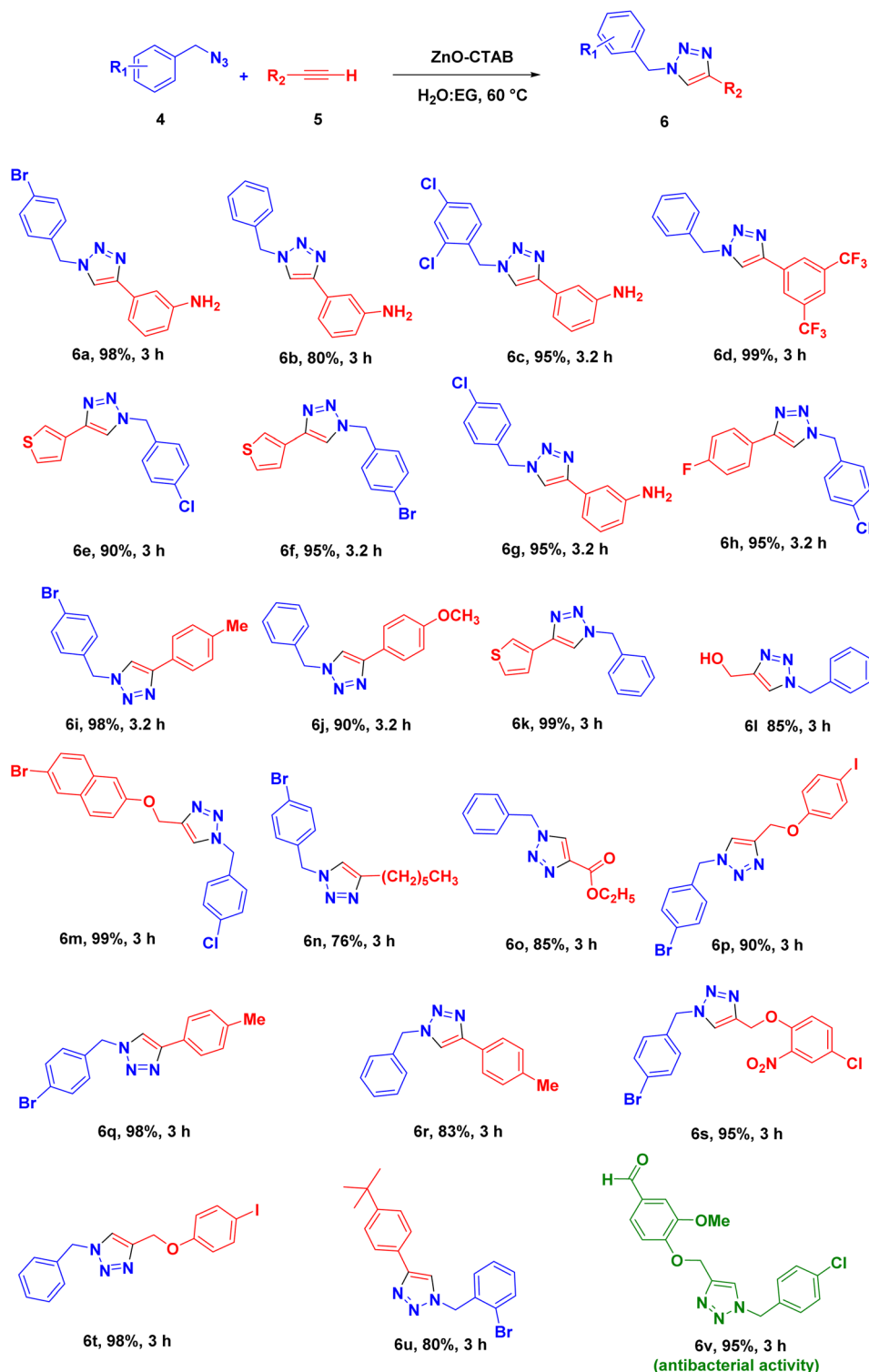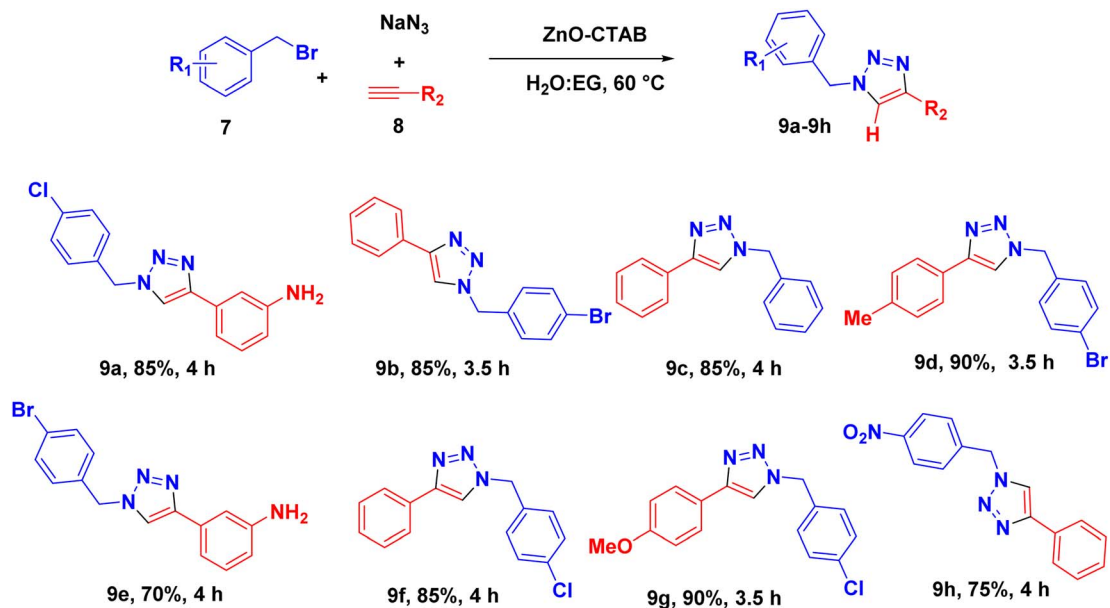
Scheme 3 ZnO-CTAB-catalyzed 1,4-disubstituted 1,2,3-triazole formation. [a]Reaction conditions: azide (1 mmol), alkynes (1.2 mmol), H$_2$O:EG (3 mL) and, catalyst (5 mg). All yields are reported as isolated yield.

afforded the required NH-triazoles with good yields and tolerated a number of aromatic aldehydes containing different functional groups (Scheme 5 and **14a–k**). Sulphur- and oxygen-containing heterocyclic aldehydes, such as thiophene-2-carboxaldehyde and furfural, reacted with ease, giving 85% and 90% yields, respectively

(Scheme 5, **14h** and **14i**). The compounds **14j** and **14k** are known to display IDO (indoleamine 2,3-dioxygenase) inhibition, which is useful in cancer treatment.[36]

Moreover, the catalyst ZnO-CTAB turned out to be efficient in the synthesis of 1,4,5-trisubstituted 1,2,3-triazoles from internally

Scheme 4 Zn-promoted 1,4-disubstituted 1,2,3-triazole formation through a one-pot three-component AAC reaction. ^{a}Reaction conditions: benzyl bromide (1 mmol), sodium azide (2 mmol), alkynes (1.2 mmol), H$_2$O:EG (3 mL), and catalyst (5 mg). All yields are reported as isolated yield.
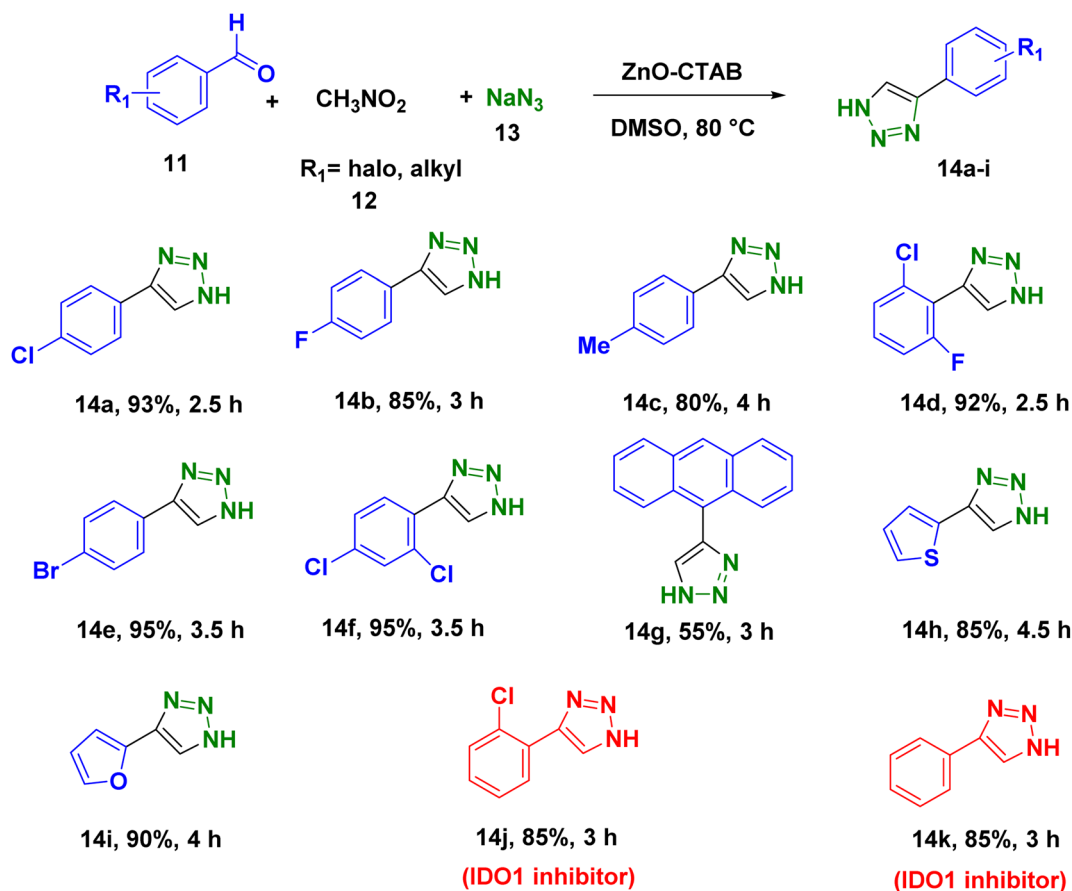
Scheme 5 Synthesis of N-unsubstituted 1,2,3-triazoles using ZnO-CTAB nanocrystals as the catalyst. ^{a}Reaction conditions: aldehyde (1 mmol), nitromethane (2 mmol) and sodium azide (3 mmol), DMSO (3 mL), catalyst (5 mg). All yields are reported as isolated yield.
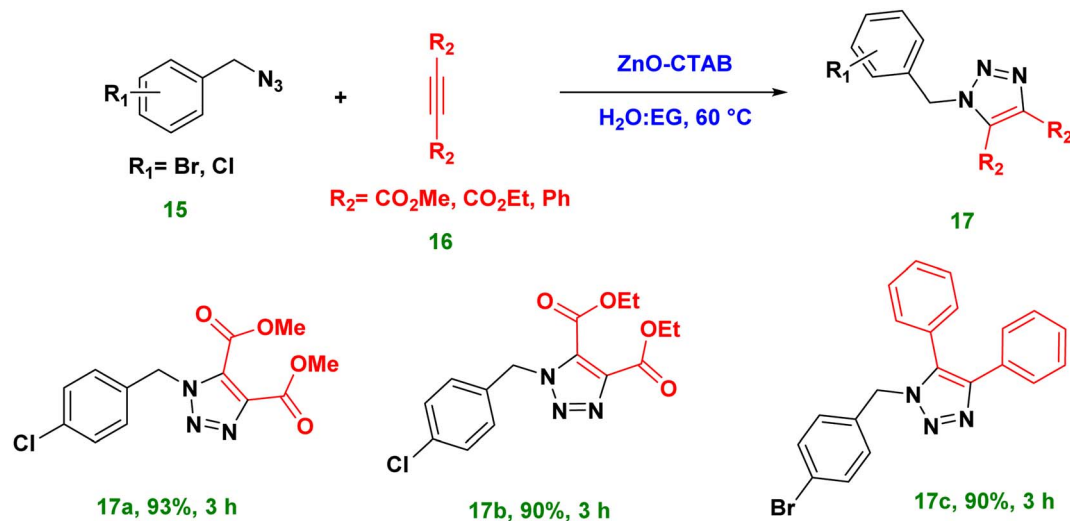
Scheme 6 Synthesis of 1,4,5-trisubstituted 1,2,3-triazoles catalyzed by ZnO-CTAB. [a]Reaction conditions: azide (1 mmol), alkynes (1.2 mmol), H$_2$O:EG (3 mL), and catalyst (5 mg). All yields are reported as isolated yield.

symmetrical alkynes. such as dimethyl acetylene dicarboxylate (DMAD), diethyl acetylene dicarboxylate and diphenylacetylene, with 90–93% yields (Scheme 6 and **17a–c**).

The structural and morphological uniqueness of the synthesized ZnO-CTAB nanoparticles, which are responsible for their outstanding catalytic performance, were by the control experiments mentioned in Table S1.† We have already discussed that commercial ZnO yielded a very low amount of the desired product with regioisomer formation in the ratio of 80 : 20 (1,4- : 1,5-). We also synthesized non-supported ZnO nanoparticles by avoiding CTAB and keeping all other reaction parameters constant, as mentioned in the experimental section, and used them as a catalyst. Interestingly, they also led to a low yield (only 60% conversion) of the required product with isomer formation at a ratio of 80 : 20. This result clearly suggests the role of particle (catalyst) size and morphology of the catalyst in product selectivity. On the other hand, when CTAB was decomposed and removed from the presynthesized ZnO-CTAB nanoparticles by calcining at 400 °C for 4 h, the newly formed ZnO without CTAB performed in a similar way, yielding only the regioselective 1,4-isomeric product (Table S1,† entry 2). This result can be attributed to the fact that the structural and morphological properties of the ZnO nanoparticles remain unchanged even after the removal of CTAB. The complete removal of CTAB from the ZnO-CTAB catalyst after calcination was verified by the FTIR spectra depicted in Fig. 5.

It is believed that the ZnO-CTAB-catalyzed cycloaddition reaction involves the formation of a metallacycle. Initially, the alkyne coordinates with the active sites *i.e.* Zn^{2+} of the catalyst by forming a π-complex, as shown in Fig. 6. This complex then co-ordinates with the azide in a particular orientation, forming the metallacycle **B**. Further, cyclization of the azides and alkynes produces the 1,4-disubstituted 1,2,3-triazoles. The metallacycle **B** favours the formation of the 1,4-adduct because, in the opposite orientation, the R group would impose steric congestion on the metallacycle, making the addition of alkyne energetically unfavourable (metallacycle **C**)[18] (Fig. 6).

The catalyst could successfully catalyze a number of reactions after recovery from preceding cycles with negligible loss, exemplifying true heterogeneity, high efficiency and stability.

For the recyclability test, the catalyst was separated from the solution after the completion of the reaction, centrifuged and washed with water and ethanol (Experimental section). Maintaining the similar molar ratio, the oven-dried catalyst was reused for four consecutive cycles (Fig. 7). Another series of experiments was performed by recovering the catalyst from the AAC reaction for disubstituted product synthesis and employed for the synthesis of *N*-unsubstituted triazoles. The recovered catalyst from this reaction was again used for preparing 1,4-disubstituted 1,2,3-triazoles *via* the one-pot reaction of 4-chlorobenzylbromide and phenylacetylene. Good yields of the desired products were obtained in all these reactions, which shows that the same catalyst can be reused for generating different types of triazole derivatives without productivity loss (Fig. 8).

Further, the recovered catalyst was characterized by PXRD analysis in order to probe any changes in the crystal structure of
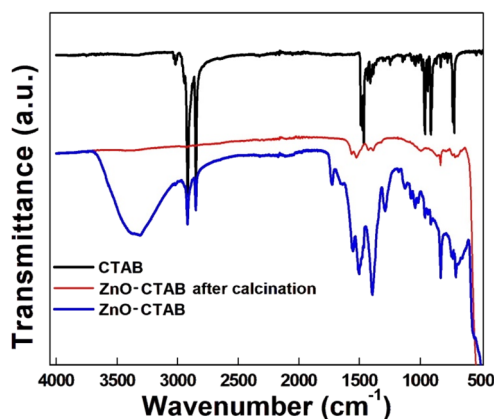

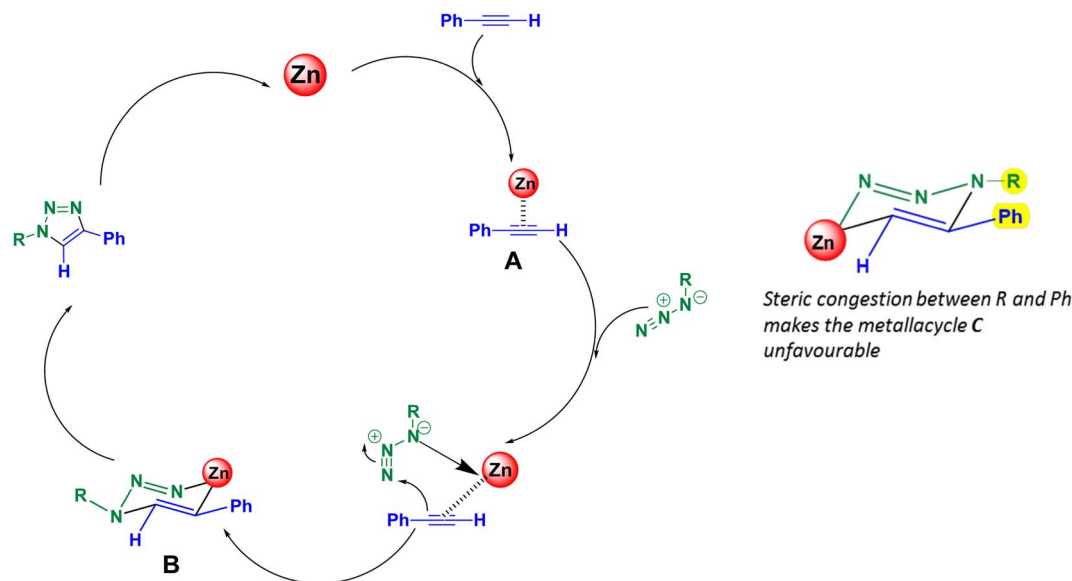**Fig. 5** FTIR spectra of pure CTAB, the as-synthesized catalyst and the calcined catalyst.

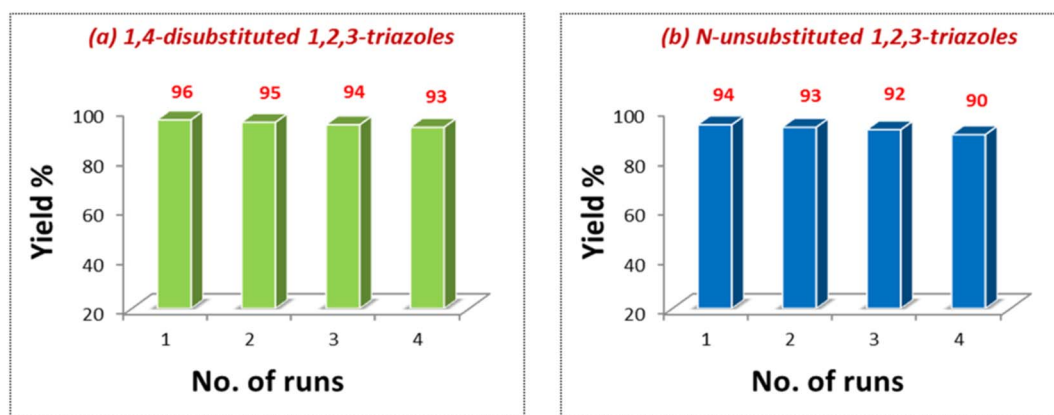**Fig. 6** Plausible mechanism of the AAC reaction catalyzed by ZnO-CTAB.

Fig. 7 Recyclability of the catalyst in the synthetic reactions of (a) 1,4-disubstituted 1,2,3-triazoles and (b) *N*-unsubstituted 1,2,3-triazoles.

the nanomaterial. No deviation was observed in the PXRD pattern of the recovered catalyst from that of the fresh catalyst, which validates the retention of structural properties in the reused catalyst (Fig. 9).

A hot filtration test was performed to investigate the leaching of the catalyst by heating 4-chloro benzyl azide and phenylacetylene along with the catalyst at 60 °C for 1.5 h, which resulted in only 40% completion of the reaction. After that, the catalyst was removed by filtration, and the remaining filtrate was tested after another 2 h. The reaction failed to proceed in the filtrate, which depicts a negative leaching test and confirms the heterogeneous nature of the developed catalyst (Fig. 9).

Gram-scale synthesis was studied by performing two individual reactions of 4-chloro benzyl azide and 4-bromobenzyl azide with phenylacetylene at 60 °C. Under the optimized reaction conditions, it produced the 1,4-isomeric product with good yields, thus marking its remarkable competence as an efficient protocol at the industrial level (Table 3, entries 15a and 15b).
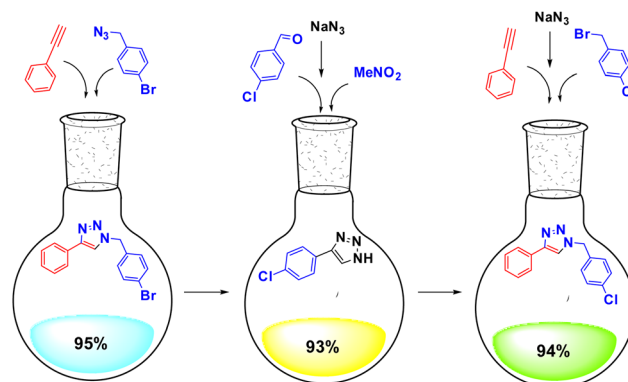

Fig. 8 Different types of 1,2,3-triazoles synthesized using the same recovered catalyst.
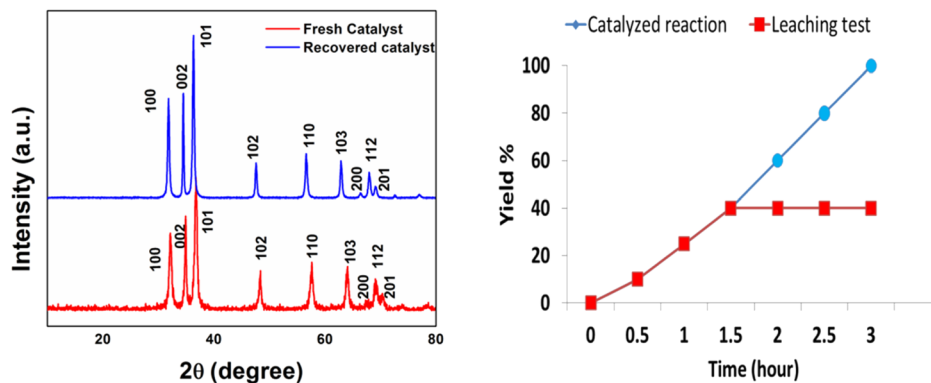
Fig. 9 XRD analysis of the fresh and recovered ZnO-CTAB nanocatalyst after the 4th cycle; hot filtration test.

Table 3 Gram-scale synthesis results

| Entry | R | Weight taken | | % yield |
		Azide	Alkyne	
15a	Cl	1 g, 4.01 mmol	0.527 g, 5.21 mmol	90
15b	Br	1 g, 6.51 mmol	0.856 g, 8.4 mmol	86

Table 4 Comparison of this work with other reported catalysts for AAC reactions

Sl. no.	Catalyst	Precursors	Reaction conditions	Yield [%]	Ref.
1	GO-Salen-Zn	Benzylbromide, phenylacetylene, sodium azide	H_2O, 100 °C, 3 h	89	39
2	CeO_2–Ag nanocomposites	Aniline, phenyl acetylene	H_2O, CeO_2–Ag, 3 h, r.t.	96	23
3	Nickel–rGO–zeolite	benzyl bromide, phenylacetylene, sodium azide	H_2O, 90 °C, 6 h	96	21
4	$Zn(OAc)_2$	4-Azidonitrobenzene and phenylacetylene	H_2O, microwave irradiation, 75 °C	97	18
5	Ag acetate complex (ligand: 2-Diphenyl phosphino-*N*,*N*-diisopropyl carboxamide)	Phenyl acetylene, benzyl azide	Caprylic acid, toluene; 90 °C, 48 h	79	41
6	Zn/C	Phenylazides, phenylacetylenes	DMF, 50 °C, 15 h	91	37
8	SiO_2@APTES@2HAP-Zn	Benzylbromide, phenylacetylene, sodium azide	H_2O:tBuOH (1 : 1), 55 °C	90	38
9	Zinc(II) L-prolinate	Aryl/alkyl-alkyne, sodium azide and aryl/alkyl/allyl halide	H_2O, reflux, 2–3 h	91	40
10	ZnO-CTAB	Benzylazide, phenylacetylene	H_2O:EG, 60 °C, 3 h	99	This work

Our methodology furnishes better efficiency in terms of catalytic conditions and yields in the AAC reactions compared with recently reported zinc-based protocols and many other recent reports (Table 4).

The atom economy, environmental factor (*E*-factor) and eco-scale were calculated for the above ZnAAC reaction, and from the results obtained, it could be concluded that the reaction has high atom economy, low environmental factor and excellent eco-score. These values confirm the eco-friendliness of our methodology (ESI, Sections 4.1–4.3†).

Conclusions

A greener inexpensive zinc-based catalyst, ZnO-CTAB, has been developed for the synthesis of both *N*-substituted and *N*-unsubstituted 1,2,3-triazole derivatives without using any base, reducing agents or ligands. The synthesized nanocrystals could catalyze the AAC reaction of various azides and alkynes possessing different functional groups to primarily form 1,4-disubstituted 1,2,3-triazole as the regioselective product *via* a one-pot method. The single-crystal XRD data of one of the product molecules confirmed the regioselectivity of the zinc-mediated AAC reaction. Moreover, the protocol was also applicable for the construction of 1,4,5-trisubstituted 1,2,3-triazoles using internal alkynes. The CTAB-supported nanorods were very stable, easy to synthesize and could be recycled up to four times for the synthesis of both the triazole derivatives, with brilliant activity in each cycle. Apart from this, the competency to generate two 1,4-disubstituted 1,2,3-triazoles in the gram scale demonstrates that this protocol is quite efficient and effective in organic synthesis.

Experimental section

Materials

Zinc acetate dihydrate [Zn(OAc)$_2$·2H$_2$O, 98.5%], cetyltrimethylammonium bromide (CTAB) and absolute ethanol (96%) were purchased from Sigma-Aldrich. Sodium hydroxide (Spectrochem), sodium azide (Spectrochem; 99% purity), nitromethane (TCI; 98% purity), all aldehydes (Spectrochem; 98% purity) and benzyl bromides (TCI and Spectrochem; 98% purity) were used directly without any further purification.

Characterization techniques

The synthesized nanocatalyst was examined by powder X-ray diffractometry (PXRD) using a Bruker D8 Advance X-ray

a JEOL (JEM-F200) instrument at an accelerating voltage of 200 kV. X-ray photoelectron spectroscopy (XPS) was carried out on an ESCALAB Xi + XPS system using an Al Kα source. The SEM and EDX analyses were carried out on a JEOL JSM-IT 300 Scanning electron microscope.

The ^{1}H NMR (500 MHz) and ^{13}C NMR (125 MHz) spectra were recorded on a Bruker Avance 500 MHz spectrometer using TMS as the internal standard. The chemical shifts of the analyzed products are presented in parts per million (ppm), and the splitting patterns are assigned as s (singlet), d (doublet), t (triplet), q (quartet), and m (multiplet). A Thermo Scientific Endura LC/MS mass spectrometer was used for recording the mass spectra of the products. ICP-MS was performed on a Thermo Fisher iCAP RQ instrument.

### Preparation of the nanostructured ZnO-CTAB catalyst

The ZnO-CTAB nanoparticles were synthesized using a simple sonochemical method. For the synthesis, an aqueous solution (10 mL) of zinc acetate dihydrate (0.219 g, 1 mmol) and cetyltrimethylammonium bromide (1.092 g, 3 mmol) was prepared by stirring till complete dissolution. Then, a 2 mmol NaOH solution was prepared in 5 mL of water and added dropwise to the zinc acetate-CTAB solution. The white precipitate formed was then stirred for 1 h followed by sonication for 60 min. The solution was then centrifuged and washed with water and ethanol to remove soluble impurities. The final solid product was then stored for further characterization.

The unsupported ZnO nanoparticles were synthesized by following the same procedure, but only the steps involving the addition of CTAB were omitted.

Synthesis of aromatic azides

To a solution of acetone and water at a 3 : 1 ratio, alkyl or benzyl bromide (10 mmol) and sodium azide (20 mmol) were added and stirred for 1 h at room temperature. The mixture was then extracted with ethylacetate and washed with water. Anhydrous sodium sulfate was added to remove any traces of water, and the solution was evaporated to obtain the required benzyl azides (9.3 mmol).

### Synthesis of 1,4-disubstituted 1,2,3-triazoles
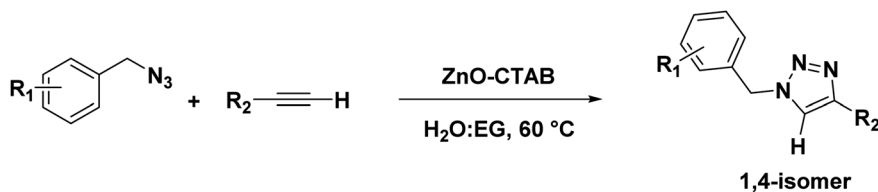
Diffractometer. Low-resolution transmission electron microscopy (TEM), selected area electron diffraction (SAED) and phase-contrast high-resolution TEM (HRTEM) were performed using

The as-synthesized catalyst (5 mg) was added to a mixture of substituted benzylazide (1 mmol) and alkyne (1.2 mmol) in an H$_2$O:EG reaction medium (6 : 1 ratio, 3 mL) at room temperature.

Then, the reaction mixture was heated in an oil bath at a constant temperature of 60 °C for 3–4 h. After that, the reaction mixture was allowed to cool, and the product was extracted by adding ethyl acetate followed by a brine solution. Anhydrous sodium sulfate was added to remove traces of water. The solvent was evaporated under reduced pressure. The final product was purified by column chromatography over silica gel using a hexane/ethyl acetate mixture, and the products obtained were characterized by NMR and mass spectroscopy.

Synthesis of *N*-unsubstituted-1,2,3-triazoles
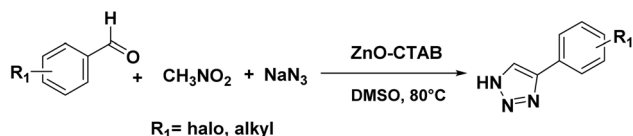
The aromatic aldehyde (1 mmol), nitroalkane (2 mmol), sodium azide (3 mmol) and catalyst (5 mg) were stirred in a round-bottom flask containing 3 mL of DMSO solvent at 80 °C. The progress of the reactions was checked by TLC. After the completion of the reaction, the mixture was cooled to room temperature and extracted with ethyl acetate (4 × 10 mL). The filtrate was evaporated to dryness under reduced pressure. The final product was purified by column chromatography over silica gel using a hexane/ethyl acetate mixture, and the products obtained were characterized by NMR and mass spectroscopy. The recovered catalyst was washed with hot ethanol, dried and reused.

Synthesis of 1,4-disubstituted 1,2,3-triazoles (one-pot method)
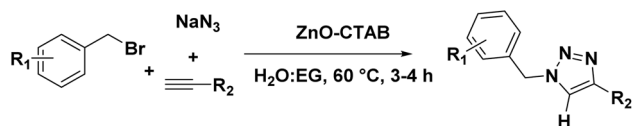
In this case, benzyl bromide (1 mmol), sodium azide (2 mmol) and phenylacetylene (1.2 mmol) were added simultaneously to a solution of water-ethylene glycol (6 : 1, 3 mL) containing the catalyst (5 mg) and reacted at 60 °C for 3–4 h. The product obtained was then extracted with ethyl acetate and purified using column chromatography. The final products were characterized by NMR and mass spectroscopy.

Synthesis of 1,4,5-trisubstituted-1,2,3-triazoles
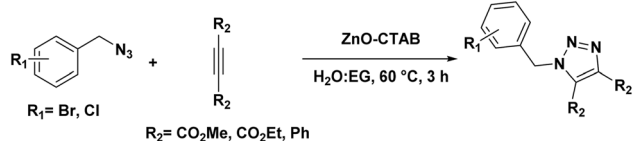
The as-synthesized catalyst (5 mg) was added to a mixture of

substituted benzylazide (1 mmol) and internal alkyne (1.2 mmol) in an H_2O:EG reaction medium (6 : 1, 3 mL). Then, the reaction mixture was heated in an oil bath at a constant temperature of 60 °C for 3 h. After that, the reaction mixture was allowed to cool, and the product was extracted by adding ethyl acetate followed by a brine solution. Anhydrous sodium sulfate was added to remove traces of water. The solvent was evaporated under reduced pressure. The final product was purified by column chromatography over silica gel using a hexane/ethyl acetate mixture, and the products obtained were characterized by NMR and mass spectroscopy.

Alkyne synthesis
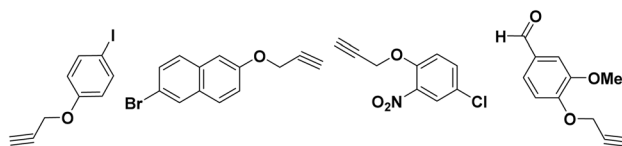
A solution of phenol (10 mmol) and K_2CO_3 (15 mmol) or Cs_2CO_3 (15 mmol) was mixed in 20 mL DMF solution in a round-bottom flask. Then, propargyl bromide was added (10 mmol) at room temperature, and the reaction mixture was stirred overnight. The final product was extracted with ethyl acetate (2 × 25 mL), washed with water and dried over Na_2SO_4. Finally, evaporation of the solvent under reduced pressure yielded the desired alkynes.

Recyclability test

To perform the recyclability test, the reaction of benzyl azide (1 mmol) and phenylacetylene (1.2 mmol) was carried out with ZnO-CTAB (5 mg) in H_2O:EG (3 mL) for 3 hours at 60 °C. After the completion of the reaction, the catalyst was separated from the solution, centrifuged and washed with water (1 mL) and ethanol (1 mL) three to four times. The recovered catalyst was dried and then reused for four consecutive reaction cycles, in which it maintained similar molar ratios of the products (Fig. 7).

In a similar way, to test catalyst recyclability in the synthesis of *N*-unsubstituted 1,2,3-triazoles, the reaction between 4-chloro benzaldehyde (1 mmol), sodium azide (3 mmol) and nitromethane (2 mmol) was performed with DMSO (3 mL) at 80 °C. After the completion of the reaction, similar centrifugation and washing steps were followed, as mentioned above. The oven-dried catalyst was then reused for four consecutive cycles, which demonstrated equivalent product molar ratios.

To assess catalyst recyclability across reactions, at first, the reaction between 4-bromo benzyl azide (1 mmol) and phenyl acetylene (1.2 mmol) was carried out with 5 mg of the catalyst in H_2O:EG (3 mL) for 3 hours at 60 °C. As the reaction was completed, the catalyst was separated from the solution, centrifuged and washed with 1 mL of water followed by 1 mL of ethanol 3–4 times. The oven-dried catalyst was then reused for the reaction of 4-chlorobenzaldehyde (1 mmol), sodium azide (3 mmol) and nitromethane (2 mmol) in DMSO (3 mL) at 80 °C.

After achieving the product, the catalyst was again recovered by following the same procedure described above and was reused for the one-pot synthesis of 1,4-disubstituted 1,2,3-triazoles using 4-chlorobenzyl bromide (1 mmol), sodium azide (2 mmol) and phenylacetylene (1.2 mmol) in H_2O:EG (3 mL) (Fig. 8).

Author contributions

P. K. H and P. G. conceptualization, data curation, formal analysis, methodology, software. S. S. data curation, methodology. B. S. analysis. K. D. and D. S. conceptualization, editing, supervision.

Conflicts of interest

There is no conflict of interest involved in this work and authors declare no competing financial interest.

Acknowledgements

References

1 J. Jampilek, *Molecules*, 2019, **24**, 3839.

2 M. M. Heravi and V. Zadsirjan, *RSC Adv.*, 2020, **10**, 44247–44311.

3 A. Kumar, K. A. Singh, H. Singh, V. Vijayan, D. Kumar, J. Naik, S. Thareja, P. J. Yadav, P. Pathak, M. Grishina, A. Verma, H. Khalilullah, M. Jaremko, H. A. Emwas and P. Kumar, *Pharmaceuticals*, 2023, **16**, 299.

4 R. K. Sharma, M. Mishra, S. Sharma and S. Dutta, *J. Coord. Chem.*, 2016, **6**, 1152–1165.

5 N. Agouram, E. M. El Hadrami and A. Bentama, *Molecules*, 2021, **26**, 2937.

6 P. Thirumurugan, D. Matosiuk and K. Jozwiak, *Chem. Rev.*, 2013, **113**, 4905–4979.

7 M. M. Alam, *Arch. Pharm.*, 2022, **355**, 2100158.

8 T. Liang, X. Sun, W. Li, G. Hou and F. Gao, *Front. Pharmacol.*, 2021, **12**, 661173.

9 L. S. Feng, M. J. Zheng, F. Zhao and D. Liu, *Arch. Pharm.*, 2021, **354**, 2000163.

10 H. M. Shaikh, D. D. Subhedar, L. Nawale, D. Sarkar, K. A. F. Khan, N. J. Sangshettic and B. B. Shingate, *MedChemComm*, 2015, **6**, 1104–1116.

11 A. Keivanloo, M. Fakharian and S. Sepehri, *J. Mol. Struct.*, 2020, **1202**, 127262.

12 N. Ashwini, M. Garg, C. D. Mohan, J. E. Fuchs, S. Rangappa, S. Anusha, T. R. Swaroopa, K. S. Rakesh, D. Kanojiab, A. Bender, H. P. Koeffler and K. S. Rangappa, *Bioorg. Med. Chem.*, 2015, **23**, 6157–6165.

13 J. Chen, T. Liang, H. Zhao, L. C. Lin and M. Chen, *Org. Biomol. Chem.*, 2019, **17**, 4843.

14 R. Huisgen, *Angew. Chem., Int. Ed.*, 1963, **2**, 565–598.

15 V. V. Rostovtsev, L. G. Green and V. V. Fokin, *Angew. Chem., Int. Ed.*, 2002, **41**, 2708–2711.

16 J. Héron and D. Balcells, *ACS Catal.*, 2022, **12**, 4744–4753.

17 G. J. Brewer, *Chem. Res. Toxicol.*, 2010, **23**, 319–326.

18 A. M. Morozova, S. M. Yusubov, B. Kratochvil, V. Eigner, A. A. Bondarev, A. Yoshimura, A. Saito, V. V. Zhdankin, E. M. Trusova and S. P. Postnikov, *Org. Chem. Front.*, 2017, **4**, 978–985.

19 N. Salam, A. Sinha, S. A. Roy, P. Mondal, R. N. Jana and M. S. Islam, *RSC Adv.*, 2014, **4**, 10001–10012.

20 P. Basu, P. Bhanjab, N. Salam, K. T. Deya, A. Bhaumik, D. Das and M. S. Islam, *Mol. Catal.*, 2017, **439**, 31–40.

21 P. Choudhury, S. Chattopadhyay, G. De and B. Basu, *Mater. Adv.*, 2021, **2**, 3042–3050.

22 P. S. H. Rao and G. Chakibanda, *RSC Adv.*, 2014, **4**, 46040–46048.

23 S. Das, P. Mondal, S. Ghosh, B. Satpati, S. Deka, S. M. Islam and T. Bala, *New J. Chem.*, 2018, **42**, 7314–7325.

24 A. A. Ali, M. Chetia, B. Saikia, P. J. Saikia and D. Sarma, *Tetrahedron Lett.*, 2015, **56**, 5892–5895.

25 M. Daraie, M. M. Heravi and N. Sarmasti, *J. Macromol. Sci., Part A: Pure Appl.Chem.*, 2020, **57**, 488–498.

26 B. Muthusamy, P. Nalenthiran, N. Muthupandi, M. Shanmugam, M. Sepperumal and B. Nattamai, *ACS Sustain. Chem. Eng.*, 2013, **1**, 1405–1411.

27 H. Ben El Ayouchia, L. Bahsis, I. Fichtali, L. R. Domingo, M. Ríos-Gutiérrez, M. Julve and S. E. Stiriba, *Catalysts*, 2020, **10**, 956.

28 J. Sultana, N. D. Khupse, S. Chakrabarti, P. Chattopadhyay and D. Sarma, *Tetrahedron Lett.*, 2019, **60**, 1117–1121.

29 P. Phukan, S. Agarwal, K. Deori and D. Sarma, *Catal. Lett.*, 2020, **150**, 2208–2219.

30 P. Gogoi, B. Bhattacharyya, V. Chakravorty, A. Garg, P. K. Hazarika, K. Deori and D. Sarma, *ChemNanoMat*, 2023, **9**, e202200407.

31 R. Kumar, G. Kumar and A. Umar, *Nanosci. Nanotechnol. Lett.*, 2014, **6**, 631–650.

32 M. Aminuzzaman, L. P. Ying, W. S. Goh and A. Watanabe, *Bull. Mater. Sci.*, 2018, **41**, 1–10.

33 P. Kiełbik, A. Jończy, J. Kaszewski, M. Gralak, J. Rosowska, R. Sapierzyński and M. M. Godlewski, *Pharmaceuticals*, 2021, **14**, 859.

34 R. Javed, M. Zia, S. Naz, S. O. Aisida, N. U. Ain and Q. J. Ao, *Nanobiotechnology*, 2020, **18**, 1–15.

35 F. Celik, R. Ustabaş, N. Süleymanoğlu, Ş. Direkel, H. İ. Gülerm and Y. Ünver, *J. Indian Chem. Soc.*, 2021, **98**, 100105.

36 Q. Huang, M. Zheng, S. Yang, C. Kuang, C. Yu and Q. Yang, *Eur. J. Med. Chem.*, 2011, **46**, 5680–5687.

37 X. Meng, X. Xu, T. Gao and B. Chen, *Eur. J. Org Chem.*, 2010, **2010**, 5409–5414.

38 R. K. Sharma, M. Mishra, S. Sharma and S. Dutta, *J. Coord. Chem.*, 2016, **69**, 1152–1165.

39 Z. Ghadamyari, A. Khojastehnezhad, S. M. Seyedi, F. Taghavi and A. Shiri, *ChemistrySelect*, 2020, **5**, 10233–10242.

40 M. Kidwai and A. Jain, *Appl. Organomet. Chem.*, 2011, **25**, 620–625.

41 J. McNulty and K. Keskar, *Eur. J. Org Chem.*, 2012, **2012**, 5462–5470.

42 Y. Pan, *CCDC 1028453: Experimental Crystal Structure Determination*, 2017.